Effects of angiotensin II intervention on MMP-2, MMP-9, TIMP-1, and collagen expression in rats with pulmonary hypertension

X.M. Wang[1], K. Shi[1], J.J. Li[2], T.T. Chen[1], Y.H. Guo[1], Y.L. Liu[1], Y.F. Yang[1] and S. Yang[1]

[1]Department of Pediatric Cardiology,
Chengdu Women's and Children's Central Hospital, Chengdu, China
[2]Department of Pediatric Rehabilitation, Zhengzhou Children's Hospital, Zhengzhou, China

Corresponding author: X.M. Wang
E-mail: wxm6910@126.com

ABSTRACT. This study investigated the effects of angiotensin II (AngII) intervention, using captopril and losartan, on the expression of matrix metalloproteinase-2 (MMP-2), MMP-9, tissue inhibitor of metalloproteinase-1 (TIMP-1), and collagen in rats with pulmonary hypertension, in an effort to understand mechanisms underlying pulmonary vascular remodeling. A total of 40 male Sprague-Dawley rats were randomly divided into normal group, model group, captopril group, and losartan group. After 5 weeks, the mean pulmonary arterial pressure (mPAP), right ventricular index, and neointima formation in each group were determined. Immunohistochemical analysis was performed to determine the degree of pulmonary arterial muscularization as well as MMP-2, MMP-9, and TIMP-1 protein expression in lung tissue. Real-time fluorescent quantitative PCR was

used to detect *MMP2*, *MMP9*, *TIMP1*, *COL1A1*, and *COL4A1* mRNA expression. Picro-sirius red staining was performed to detect collagen protein expression. Neointima formation was observed in the model group. Moreover, the mPAP, right ventricular index, degree of arterial muscularization, and collagen deposition, as well as mRNA and protein expression of *MMP2*, *MMP9*, and *TIMP1* were significantly higher than those in the other groups (P < 0.05). The mPAP, right ventricular index, degree of arterial muscularization, and mRNA and protein expression in the captopril and losartan groups were significantly decreased compared with those of the model group (P < 0.05). AngII regulates MMP-2, MMP-9, and TIMP-1 expression and affects collagen deposition. Thus, this hormone is involved in pulmonary vascular remodeling, indicating a possible mechanism that can be targeted in pulmonary hypertension intervention.

Key words: AngII; MMP-2; MMP-9; Pulmonary hypertension; TIMP-1

INTRODUCTION

Vascular remodeling is a common feature of pulmonary hypertension (PAH) and involves reconstruction of the intima, tunica media, tunica adventitia, and extracellular matrix (ECM) reconstructions. ECM remodeling involves collagen and elastin deposition, which promotes the reconstruction of the tunica adventitia. Matrix metalloproteinases (MMPs) are ECM proteolytic enzymes that are involved in collagen degradation, particularly of collagen I and collagen IV; MMPs also serve important functions in ECM formation, cell migration, and growth regulation (Rubin, 2002; Hassoun, 2005). Investigating the functions of MMPs in pulmonary vascular remodeling (PVR) may help to elucidate the mechanism underlying PAH.

Angiotensin II (AngII) is a protein factor that promotes the proliferation of vascular smooth muscle cells (VSMCs) and strongly induces mitosis. Numerous studies have been conducted on the role of AngII in PAH. However, studies on the relationship between AngII and MMPs have not been reported to date. This study utilizes the left pneumonectomy + monocrotaline (MCT) PAH model to investigate the relationship between MMPs and AngII and to elucidate the mechanism of action of AngII in PAH.

MATERIAL AND METHODS

Animals and grouping

This study was carried out in strict accordance with the recommendations stipulated in the Guide for the Care and Use of Laboratory Animals of the National Institutes of Health. The animal use protocol was reviewed and approved by the Institutional Animal Care and Use Committee (IACUC) of Chengdu Women's and Children's Central Hospital.

A total of 40 healthy male Sprague-Dawley rats with weights ranging from 350 to 400 g were provided by the Animal Testing Center, Sichuan University, China. Larger animals were chosen to minimize the effects of growth and development on vascular remodel-

ing. Moreover, MCT-induced inflammation decreases with increasing age (Nishimura et al., 2001). The rats were randomly divided into the following four groups, with 10 rats in each group: normal group (NG), left lung resection + MCT group (model group, MG), captopril group (CG), and losartan group (LG). The NG group did not receive any treatment. In the MG group, MCT (Sigma-Aldrich, St. Louis, MO, USA) was injected subcutaneously 1 week after left pneumonectomy. In the CG group, 10 mg·kg^{-1}·day^{-1} captopril (Sino-American Shanghai Squibb Pharmaceuticals Ltd., Shanghai, China) was administered 3 days prior to the operation. In the LG group, 15 mg·kg^{-1}·day^{-1} losartan (Hangzhou MSD Pharmaceutical Company Ltd., Hangzhou, China) was administered 3 days prior to the operation.

Animal modeling

Left pneumonectomy was performed according to the methods described in the literature (Nishimura et al., 2001), with the following modifications: rats received intramuscular injections of atropine in the right hind limb (50 μg/kg) and subsequent intraperitoneal injections of 10% chloral hydrate (0.04 mL/kg), 20 min later. After administration of anesthesia, endotracheal intubation was performed using a 2-mm ID catheter under naked-eye observation. An HX200 small-animal ventilator (Chengdu Taimeng Science and Technology Co., Ltd., Chengu, China) was used to maintain ventilation (tidal volume: 3 mL; inspiratory-to-expiratory ratio: 1:2; respiratory rate, 60 bpm). Under aseptic conditions, the chest wall and pleural cavity were incised along the left 5th intercostal space. The left-lung hilum was separated and ligated, while avoiding ligation of nerves. The left lung was subsequently removed. A small amount of saline solution was used to rinse the stump, and the chest wall was closed layer by layer. Rat breathing was then monitored. When the breathing rhythm was smooth and no obvious dyspnea was observed, extubation was performed. When significant dyspnea was observed, extubation was delayed. Postoperative oxygen aspiration was performed on all animals for 24 h (2 L·min^{-1}·cage^{-1}), after which normoxia aspiration was applied. After 1 week, the rats were subcutaneously injected with MCT (60 mg/kg). The animals were sacrificed 5 weeks after the surgery (i.e., 4 weeks after MCT injection).

All animals had free access to water and food. Breeding sanitation was ensured, and suitable temperature and humane management were provided.

Determination of mean pulmonary artery pressure (mPAP)

After intraperitoneal anesthesia with 10% chloral hydrate, as before, catheterization of the rat external jugular vein was performed. A PM-8000 multiparameter monitor (Shenzhen Mindray Bio-Medical Electronics Co., Ltd.) was used to measure mPAP.

Heart weight determination

Animals were sacrificed after mPAP determination, and the heart and lung were dissociated. The atria and major vessels were then removed from the heart, and the right ventricle (RV) and left ventricle plus septum (LV + S) were collected. After washing off the blood, surface moisture was absorbed with a filter paper. An electronic scale was used to weigh the tissue, and the right cardiac index was calculated using the formula RV / (LV + S).

Preparation of lung tissues

The blood remaining on the right lung was washed off by passing a saline solution through the lung artery. At the same time, 10% neutral formalin was slowly injected into the lung through the trachea under 20 cmH$_2$O pressure (Tang et al., 2004) to expand the lung membrane smoothly. After 5 min, the right lower lung lobe was cut, fixed in 10% neutral formalin by immersion for 48 h, and subsequently embedded in paraffin. Serial sections (5 μm thick) were then prepared and stained with hematoxylin and eosin (HE) and Van Gieson staining.

Degree of muscularization of non-myogenous vessels

The immunohistochemical LsAB method was used to stain α-actin with an antibody obtained from Boster Biological Technology Ltd. The α-actin-stained slices were observed under a light microscope at 400X magnification. Ten small arteries with diameters ranging from 15 to 50 μm per slice were randomly selected and observed. Positive α-actin staining indicated muscularization. The degree of muscularization was calculated using the following formula:

Muscularization degree (%) = (number of complete muscularized vessels + number of partially muscularized vessels) / 1 x 100%.

Neointimal observation

The Van Gieson elastic fiber method was used to stain the sections. Pulmonary arteries (15 to 150 μm) were observed under a light microscope at 400X magnification. The neointima was located between the inner side of the elastic lamina and outside the endothelial cells.

Immunohistochemistry

Paraffin sections of pulmonary tissues were stained using the immunohistochemical LsAB-staining method, with an antibody obtained from Boster Biological Technology Ltd. PBS replaced the primary antibody as the negative control. Cells showing uniform brown particles in the cytoplasm or membranes were considered positive, whereas cells lacking brown particles were considered negative as reported elsewhere (O'Driscoll et al., 1999; Jacobs et al., 2001). The Image-Pro Plus image analysis software (Version 4.1, Media Cybernetics Co., Ltd., USA) was used. All slices were uniformly magnified (10 x 40) under the light microscope for analysis. For each slice, five fields were randomly chosen, using equidistant sampling, and were inputted into the computer as measurement fields. Semiquantitative analysis was performed using integrated optical density.

Picro-sirius red staining

According to a previously described method (Zhang et al., 2006), lung-tissue paraffin sections were conventionally dewaxed and replaced with water. A saturated Sirius red-picric acid solution (Sigma-Aldrich) was used for the staining. A polarized light microscope (Nikon, Tokyo, Japan) was used to observe the samples. The presence of collagen was determined by the appearance of a double refraction. Collagens I to IV were differentiated based on the different colors and characteristic density of arrangement.

QF-PCR

mRNA was extracted from frozen lung tissues using Trizol according to manufacturer instructions. The integrity of the extracted RNA was determined using agarose gel electrophoresis. Afterwards, the extracts were stored at -70°C. cDNA was prepared from the mRNA using a RevertAid™ First-Strand cDNA Synthesis Kit according to manufacturer instructions and was performed by MBI Co., Ltd. (Lithuania). The synthesized cDNA was either used for PCR amplification or stored at -20°C until required.

Primers were designed to the gene sequences of rat *MMP2*, *MMP9*, *TIMP1*, *COL1A1*, *COL4A1*, and *GAPDH* in NCBI GenBank. For *MMP2*, the upstream primer was 5'-GAGTTGGCAGTGCAATACCT-3', and the downstream primer was 5'-CCAAAGAACT TCTGCATCTTCT-3'; the amplicon length was 104 bp. For *MMP9*, the upstream primer was 5'-CTTCGAGGGCCACTCCTACT-3', and the downstream primer was 5'-CAGTGACGTCGGCTCGAGT-3'; the amplicon length was 129 bp. For *TIMP1*, the upstream primer was 5'-GCAACTCGGACCTGGTTAT-3', and the downstream primer was 5'-GTCGAATCCTTTGAGCATCTT-3'; the amplicon length was 113 bp. For *COL1A1*, the upstream primer was 5'-ATCAAGGTCTACTGCAACAT-3', and the downstream primer was 5'-CAGGATCGGAACCTTCGCTT-3'; the amplicon length was 123 bp. For *COL4A1*, the upstream primer was 5'-CGCTGCGAAGGGTGATTGT-3', and the downstream primer was 5'-AAAAGGGTGATGCTGGAGAAC-3'; the amplicon length was 129 bp. For *GAPDH*, the upstream primer was 5'-CCTCAAGATTGTCAGCAAT-3', and the downstream primer was 5'-CCATCCACAGTCTTCTGAGT-3'; the amplicon length was 141 bp. The primers were synthesized and qualitatively approved by TaKaRa Co., Ltd. (Japan). SYBR Green I fluorophore was added into the PCR mixture, and the reaction was performed using a FTC2000 QF-PCR instrument. The following reaction conditions were used: denaturation at 94°C for 2 min, followed by denaturation at 94°C for 20 s; annealing at 55°C for 30 s, and extension at 72°C for 40 s, and 45 cycles were performed. During PCR, a blank tube lacking cDNA was used as the negative control.

Analysis of results

One cDNA sample was subjected to a 10-fold serial dilution, and PCR amplification was performed as described above. The logarithm of the sample copy was set as the abscissa, and the Ct value (which is the number of cycles when the fluorescent signal in each reaction tube reached the set threshold value) was set as the ordinate. QF-PCR standard curves for *MMP2*, *MMP9*, *TIMP1*, *COL1A1*, *COL4A1*, and *GAPDH* were then fitted. The $-\Delta\Delta^{Ct}$ approach (Livak and Schmittgen, 2001) was used to quantify the gene expression levels for statistical analysis.

Statistical analysis

Data are reported as means ± SD. Analysis of variance was performed using $\alpha = 0.05$. The SPSS13.0 software package was used for the statistical analysis.

RESULTS

mPAP, RV/LV + S, and degree of muscularization of non-myogenous vessels

The mPAP, RV/LV + S, and degree of muscularization in the MG group were significantly higher (P < 0.05) than those in the other three groups. No significant differences were observed between CG and LG groups. However, significant differences were found when these two groups were compared with the MG and NG groups (P < 0.05; Table 1).

Table 1. Comparison of mPAP, RV/LV + S, and degree of muscularization of the non-myogenous vessels (means ± SD, N = 10).

Groups	mPAP (mmHg)	RV/LV + S (%)	Muscularization degree (%)
MG (model)	39.30 ± 2.541*	62.25 ± 3.47[Δ]	69.33 ± 4.35[α]
CG (captopril)	24.10 ± 2.601**	48.80 ± 4.63[ΔΔ]	48.26 ± 3.65[αα]
LG (losartan)	23.10 ± 2.025**	49.06 ± 4.36[ΔΔ]	50.34 ± 2.84[αα]
P	<0.05	<0.05	<0.05

Analysis of variance was performed for intergroup comparison of the indicators: *compared with the other groups, P < 0.05, **compared with NG and MG, P < 0.05; [Δ]compared with the other groups, P < 0.05, [ΔΔ]compared with NG and MG, P < 0.05; [α]compared with the other groups, P < 0.05, [αα]compared with NG and MG, P < 0.05.

Pulmonary artery neointima formation

The results of the Van Gieson elastic fiber staining show that the vascular walls of the small arterioles in the MG group were significantly thicker than those in the other groups. Moreover, the lumina of the MG group were smaller, and neointima formation was clearly observed. In the CG and LG groups, the vascular walls of the small arterioles were thickened compared with those of the NG group, but were thinner than those in the MG group (Figure 1).
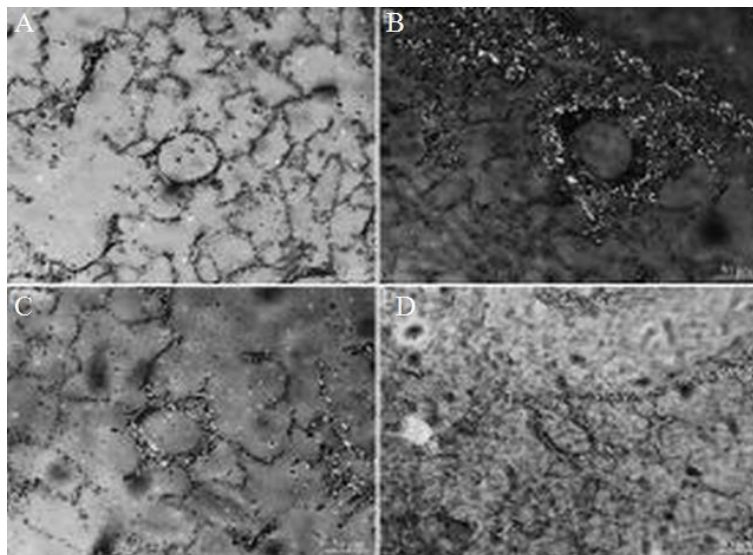
Figure 1. Pulmonary artery neointima formation. **A.** Normal group; **B.** left lung resection + MCT group; **C.** captopril group; **D.** losartan group (400X).

MMP-2, MMP-9, and TIMP-1 protein expression

MMP-2, MMP-9, and TIMP-1 expression was significantly higher in the MG group than in the other groups ($P < 0.01$). No significant differences were observed between the CG and LG groups. However, significant differences were found when these two groups were compared with the MG and NG groups ($P < 0.01$; Table 2).

Table 2. IOD comparison of MMP-2, MMP-9, and TIMP-1 expression in each group (means ± SD, N = 10).

Groups	MMP-2	MMP-9	TIMP-1
NG	25.59 ± 2.01	28.02 ± 7.17	23.71 ± 4.74
MG	128.1 ± 9.05*	107.50 ± 16.72*	131.60 ± 19.06*
CG	76.47 ± 4.61**	65.29 ± 7.17**	61.91 ± 7.37**
LG	74.23 ± 10.04**	62.63 ± 13.07**	63.30 ± 11.37**

*$P < 0.05$ and **$P < 0.01$, compared with NG; *$P < 0.01$, compared with the other groups.

MMP2, *MMP9*, and *TIMP1* mRNA expression

MMP2, *MMP9*, and *TIMP1* mRNA expression in MG were significantly higher than that in the other groups ($P < 0.01$). No significant differences were observed between the CG and LG groups. However, significant differences were found when these two groups were compared with the MG and NG groups ($P < 0.01$; Table 3).

Table 3. mRNA expression of *MMP2*, *MMP9*, and *TIMP1* (-$\Delta\Delta^{Ct}$ value, means ± SD, N = 10).

| Groups	*MMP2*	*MMP9*	*TIMP1*
NG	-6.36 ± 0.66	-6.05 ± 0.78	-5.92 ± 0.71
MG	-1.77 ± 1.03	-1.05 ± 1.12$^{\Delta}$	-1.35 ± 1.20
CG	-3.15 ± 0.98**	-3.20 ± 0.87$^{\Delta\Delta}$	-3.17 ± 1.01
LG	-3.30 ± 0.75**	-3.15 ± 0.82$^{\Delta\Delta}$	-3.10 ± 0.91
P	<0.01	<0.01	<0.01

Analysis of variance was performed for intergroup comparison of the indicators: **compared with NG and MG, $P < 0.05$; $^{\Delta}$compared with the other groups, $P < 0.05$, $^{\Delta\Delta}$compared with NG and MG, $P < 0.05$.

Collagen distribution and expression

In all groups, collagen was distributed in the interstitia of the lung tissues and in the adventitia of small blood vessels. Moreover, the collagen content in the MG group was higher than those in the other groups. Collagen type I fibers were red or yellow and were densely arranged. These fibers exhibited strong refraction. In contrast, the base film of the type IV fibers was light yellow, and the fibers exhibited weak double refraction (Figure 2).

COL1A1 and *COL4A1* mRNA expression

COL1A1 and *COL4A1* mRNA expression in the MG group was significantly higher than those in the other groups ($P < 0.05$). No significant differences were observed between the CG and LG groups. However, significant differences were found when these two groups were compared with the MG and NG groups ($P < 0.05$; Table 4).
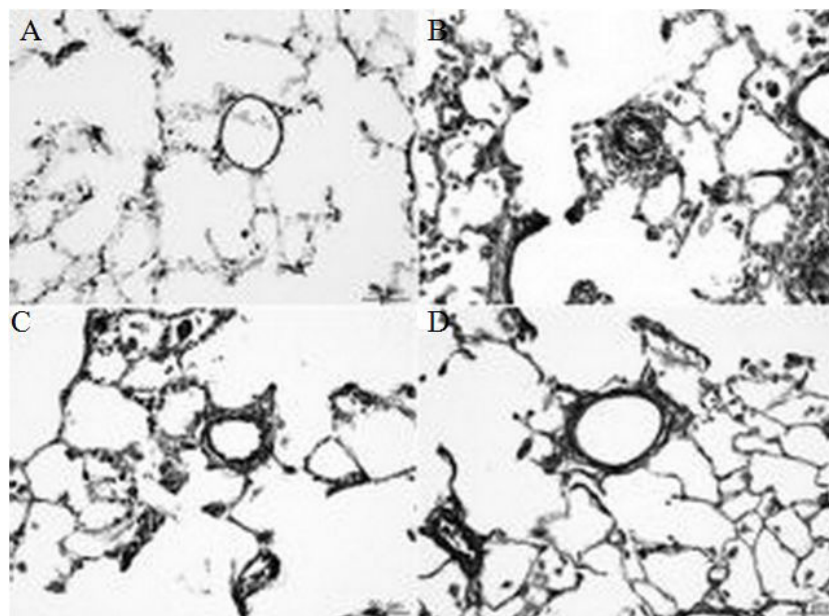
Figure 2. Distribution and expression of collagen (picro-sirius red staining). **A.** Normal group; **B.** left lung resection + MCT group; **C.** captopril group; **D.** losartan group.

Table 4. mRNA expression of *COL1A1* and *COL4A1* ($-\Delta\Delta^{Ct}$ value, means ± SD, N = 10).

Groups	COL1A1	COL4A1
NG	-5.2 ± 0.76	-3.8 ± 0.67
MG	-1.1 ± 0.82*	-0.8 ± 0.57$^\Delta$
CG	-3.0 ± 0.50**	-2.6 ± 0.65$^{\Delta\Delta}$
LG	-2.8 ± 0.45**	-2.1 ± 0.66$^{\Delta\Delta}$
P	<0.05	<0.05

Analysis of variance was performed for intergroup comparison of the indicators: *compared with the other groups, $P < 0.05$, **compared with NG and MG, $P < 0.05$; $^\Delta$compared with the other groups, $P < 0.05$, $^{\Delta\Delta}$compared with NG and MG, $P < 0.05$.

DISCUSSION

The pathological mechanism of PAH is highly complex. The central part of this process is PVR, which is induced by vascular endothelial injury and overproliferation of smooth muscle cells (SMCs) (Simonneau et al., 2009; Beghetti et al., 2010). Vascular endothelial cell dysfunction and abnormal proliferation of SMCs both lead to abnormal contraction of pulmonary vessels and reconstruction of the distal pulmonary artery, which are followed by pathological changes, such as medial hypertrophy, intimal hyperplasia, neointima formation, intimal fibrosis, plexiform lesions, and thrombosis (Brudford et al., 2010). Current studies suggest that a possible PVR mechanism includes increased pulmonary blood flow, vascular endothelial cell injury, phenotypic changes in SMCs, excessive cell proliferation, decreased apoptosis, pulmonary vascular bed remodeling, and luminal narrowing (Lévy et al., 2007).

Of these, the most important facet is the change in ECM components, which mainly includes increased synthesis of elastin and collagen proteins and their abnormal deposition in pulmonary vascular walls (Heath and Edwards, 1958). Under normal conditions, a balance exists between the factors inhibiting and stimulating SMC growth. These factors are responsible for the synthesis and release of pulmonary vascular endothelial cells. When the body is stimulated by damaging factors, vascular endothelial cells become impaired, and the balance is disrupted. Consequently, the production and expression of VSMC proliferation-promoting cytokines significantly increase and results in the abnormal proliferation of vascular smooth muscles, activation of fibroblasts, and release of inflammatory cytokines. In turn, pulmonary vascular resistance increases and subsequently induces PVR, which eventually leads to the development of PAH (Morrell et al., 2009).

AngII is a VSMC proliferation-promoting factor that exhibits strong mitogenic effects. AngII acts on the AngII type I receptor (AT_1R) and generates two types of enzymes, namely, P44MAPK and P42MAPK. P44MAPK and P42MAPK activate G protein and protein kinase C, increase intracellular calcium, and initiate DNA synthesis; these processes sustain cell proliferation and exert various effects on VSMCs (Schiffrin and Touyz, 2004). Animal studies have suggested that, in PAH, the RAS is activated and the activities of lung tissue AngII increase (Orte et al., 2000). Moreover, some studies have demonstrated that inhibition of AngII activity could reduce PAH and PVR (Yamazato et al., 2009; Shenoy et al., 2011). Excessive activation of the RAS can damage endothelial cells and so result in PVR (Zhong et al., 2011).

Studies have shown that AngII activation plays a crucial role in pulmonary fibrosis (Budinger, 2011), and that fibrosis is a vital component of ECM changes; thus, one possible mechanism for AngII-induced PVR is via vessel fibrosis (Intengan and Schiffrin, 2001), which is mainly due to ECM deposition (particularly of collagen) on the arterial walls. AngII can activate the formation of VSMC-1 collagen via the MAPK pathway (mediated by AT_1R).

MMPs constitute a major protease family that regulates ECM remodeling. MMPs may be involved in the turn-over of the ECM as well as in the migration of SMCs and the migration and proliferation of endothelial cells. MMPs can also regulate the deposition of ECM proteins on resistance vessels. Gelatinase-MMP-2 and gelatinase B (gelatinase-MMP-9) can degrade denatured collagen, including collagens IV and V, and particularly collagen IV, as well as promote SMC proliferation and migration; MMPs may also be involved in collagen IV reversal (George et al., 2012). To date, numerous studies have shown that increased MMP expression is a significant factor in PAH and PVR (Schumann et al., 2010; Jiang et al., 2012). A number of studies have also suggested a correlation between MMP expression and RAS activation (Dab et al., 2011). Therefore, future studies should focus on investigating the relationships between AngII, MMPs, and collagen to elucidate the function of AngII in PAH and to facilitate understanding of the mechanisms underlying PVR. Current studies investigating the relationship between MMP and PAH mainly focus on hypoxic PAH animal models and seldom use the MCT model. However, these models do not consider the damage caused by severe PAH-induced neointima formation.

In this study, we investigated the relationships between AngII, MMPs, and collagen and their involvement in rat PAH. The model used considered severe PAH-induced neointima by including the left pneumonectomy + MCT treatment. This model is highly suitable for mimicking severe PAH. The mPAP, RV/LV + S, and degree of muscularization of myogenous vessels due to this treatment were significantly increased compared with those of the NG group. Neointima formation was also observed in the MG group.

The QF-PCR and immunohistochemistry results of this study showed that MMP-2, MMP-9, and TIMP-1 protein expression in the MG group was significantly higher than that in the other groups. Use of an angiotensin-converting enzyme inhibitor (captopril) and AT_1R blocker (losartan) inhibited the expression of the aforementioned proteins; however, the expression levels remained significantly higher than those of the NG group, indicating that AngII can induce MMP-2, MMP-9, and TIMP-1 expression. In contrast, captopril and losartan could block the AngII effect through different channels, and thus significantly reduce the mPAP, RV/LV+S, and degree of muscularization of myogenous vessels. In turn, PVR is then inhibited, and the desired therapeutic effect is achieved.

Collagens are major components of the ECM. Collagens can be classified into interstitial collagen, basilemmal collagen, and pericellular collagen, depending on their properties and distribution in the body. Type I, II, and III collagens are interstitial, whereas type IV collagen is basilemmal (Conchman et al., 1994). Our study showed that AngII can promote the mRNA expression of *COL1A1* and *COL4A1*. Picro-sirius red staining revealed deposition of collagen in the pulmonary vascular adventitia and lung interstitial tissues, whereas MMP was shown to degrade ECM collagen. Expression of both collagens α1-I and α1-IV increased, suggesting that PVR is a complex, dynamic process involving the simultaneous synthesis and decomposition of multiple factors.

MMP-2 and MMP-9 can degrade components of basilemmal membranes, mainly type IV collagen, promote the proliferation and migration of SMCs, and participate in the turn-over of type IV collagen (Frisdal et al., 2001). The MMP/TIMP ratio is an accurate indicator of lung tissue repair and determines PVR progress (Li et al., 2011; Tang et al., 2011). Our results show that MMP-2, MMP-9, and TIMP-1 expression levels increased, which implies a dynamic, balanced relationship between MMP and its specific tissue inhibitors. A disruption in this balance by related factors affects the process of PVR. Our findings suggested that angiotensin-converting inhibitors and AT_1R blockers can interfere with the expression of MMP-2, MMP-9, and TIMP-1 by inhibiting the action of AngII. This inhibition affects collagen deposition and delays PVR.

REFERENCES

Beghetti M and Tissot C (2010). Pulmonary hypertension in congenital shunts. *Rev. Esp. Cardiol.* 63: 1179-1193.

Brudford CN, Ely DR and Raizada MK (2010). Targeting the vasoprotective axis of the renin-angiotensin system: a novel strategic approach to pulmonary hypertensive therapy. *Curr. Hypertens. Rep.* 12: 212-219.

Budinger GR (2011). Angiotensin II and pulmonary fibrosis, a new twist on an old story. *Am. J. Physiol. Lung Cell. Mol. Physiol.* 301: L267-L268.

Conchman JR, Beavan LA and McCarthy KJ (1994). Glomerular matrix: synthesis, turnover and role in mesangial expansion. *Kidney Int.* 45: 328-335.

Dab H, Hachani R, Hodroj W, Sakly M, et al. (2011). Interaction between sympathetic nervous system and renin angiotensin system on MMPs expression in juvenile rat aorta. *Gen. Physiol. Biophys.* 30: 271-277.

Frisdal E, Gest V, Vieillard-Baron A, Levame M, et al. (2001). Gelatinase expression in pulmonary arteries during experimental pulmonary hypertension. *Eur. Respir. J.* 18: 838-845.

George J, Sun J and D'Armiento J (2012). Transgenic expression of human matrix metalloproteinase-1 attenuates pulmonary arterial hypertension in mice. *Clin. Sci.* 122: 83-92.

Hassoun PM (2005). Deciphering the "matrix" in pulmonary vascular remodeling. *Eur. Respir. J.* 25: 778-779.

Heath D and Edwards JE (1958). The pathology of hypertensive pulmonary vascular disease: a description of six grades of structural changes in the pulmonary arteries with special references to congenital cardiac defects. *Circulation* 18: 533-547.

Intengan HD and Schiffrin EL (2001). Vascular remodeling in hypertension roles of apoptosis, inflammation, and fibrosis. *Hypertension* 38: 581-587.

Jacobs JJ, Lehé C, Cammans KD, Yoneda K, et al. (2001). An automated method for the quantification of immunostained

human Langerhans cells. *J. Immunol. Methods* 247: 73-82.

Jiang L, Zhou T and Liu H (2012). Combined effects of the ATP-sensitive potassium channel opener pinacidil and simvastatin on pulmonary vascular remodeling in rats with monocrotaline-induced pulmonary arterial hypertension. *Pharmazie* 67: 547-552.

Lévy M, Maurey C, Celermajer DS, Vouhé PR, et al. (2007). Impaired apoptosis of pulmonary endothelial cells is associated with intimal proliferation and irreversibility of pulmonary hypertension in congenital heart disease. *J. Am. Coll. Cardiol.* 49: 803-810.

Li XQ, Wang HM, Yang CG, Zhang XH, et al. (2011). Fluoxetine inhibited extracellular matrix of pulmonary artery and inflammation of lungs in monocrotaline-treated rats. *Acta Pharmacol. Sin.* 32: 217-222.

Livak KJ and Schmittgen TD (2001). Analysis of relative gene expression data using real-time quantitative PCR and the 2(-Delta Delta Ct) method. *Methods* 25: 402-408.

Morrell NW, Adnot S, Archer SL, Dupuis J, et al. (2009). Cellular and molecular basis of pulmonary arterial hypertension. *J. Am. Coil. Cardiol.* 54: S20-S31.

Nishimura T, Faul JL, Berry GJ, Veve I, et al. (2001). 40-O-(2-hydroxyethyl)-rapamycin attenuates pulmonary arterial hypertension and neointimal formation in rats. *Am. J. Respir. Crit. Care Med.* 163: 498-502.

O'Driscoll SW, Marx RG, Fitzsimmons JS and Beaton DE (1999). Method for automated cartilage histomorphometry. *Tissue Eng.* 5: 13-23.

Orte C, Polak JM, Haworth SG, Yacoub MH, et al. (2000). Expression of pulmonary vascular angiotensin-converting enzyme in primary and second plexiforill pulmonary hypertension. *J. Pathol.* 192: 379-384.

Rubin LJ (2002). Therapy of pulmonar hypertension: the evolution from vasodilators to antiproliferative agents. *Am. J. Respir. Crit. Care Med.* 166: 1308-1309.

Schiffrin EL and Touyz RM (2004). From bedside to bench to bedside: role of renin-angiotension-aldosterone system in remodeling of resistance arteries in hypertension. *Am. J. Physiol. Heart Physiol.* 287: 435-447.

Schumann C, Lepper PM, Frank H, Schneiderbauer R, et al. (2010). Circulating biomarkers of tissue remodelling in pulmonary hypertension. *Biomarkers* 15: 523-532.

Shenoy V, Qi Y, Katovich MJ and Raizada MK (2011). ACE2, a promising therapeutic target for pulmonary hypertension. *Curr. Opin. Pharmacol.* 1l: 150-155.

Simonneau G, Robbins IM, Beghetti M, Channick RN, et al. (2009). Updated clinical classification of pulmonary hypertension. *J. Am. Coll. Cardiol.* 30: S43-S54.

Tang JR, Markham NE, Lin YJ, McMurtry IF, et al. (2004). Inhaled nitric oxide attenuates pulmonary hypertension and improves lung growth in infant rats after neonatal treatment with a VEGF receptor inhibitor. *Am. J. Physiol. Lung Cell. Mol. Physiol.* 287: L344-L351.

Tang WL, Guo H, Yang J, Chen B, et al. (2011). Suppression of tissue inhibitors of metalloproteinases may reverse severe pulmonary arterial hypertension. *Cytotherapy* 13: 499-502.

Yamazato Y, Ferreira AJ, Hong KH, Sriramula S, et al. (2009). Prevention of pulmonary hypertension by Angiotensin-converting enzyme 2 gene transfer. *Hypertension* 54: 365-371.

Zhang H, Sun L, Wang W and Ma X (2006). Quantitative analysis of fibrosis formation on the microcapsule surface with the use of picro-sirius red staining, polarized light microscopy, and digital image analysis. *J. Biomed. Mater. Res. A* 76: 120-125.

Zhong J, Guo D, Chen CB, Wang W, et al. (2011). Prevention of angiotensin II-mediated renal oxidative stress, inflammation, and fibrosis by angiotensin converting enzyme 2. *Hypertension* 57: 314-322.